Effect of morphology on electron drift mobility in porous TiO_2

B. O. Aduda,[1,†] P. Ravirajan,[2] K. L. Choy,[3] and J. Nelson[2]

[1] *Department of Materials, Imperial College London, SW7 2BP, UK*

[2] *Centre for Electronic Materials and Devices, Department of Physics, Imperial College London, SW7 2BZ, UK*

[3] *School of Mechanical, Materials, Manufacturing Engineering and Management, University of Nottingham, Nottingham NG7 2RD, UK*

ABSTRACT. Porous titanium dioxide is an attractive material for solar cell application on account of its stability, electron transport properties, and the possibilities for controlling surface morphology as well as for its ease of fabrication and low cost. Nanostructured TiO_2 has been intensively studied for applications to dye sensitised solar cells. The performance of the titanium dioxide based solar cells is influenced, among other factors, by the electron mobility of the porous titanium dioxide. Different fabrication processes for porous titanium films result in different film morphology, which in turn affects the electron transport. We have employed three different techniques namely, electrostatic spray assisted vapour deposition (ESAVD), D.C. reactive sputtering, and doctor blading of sol-gel dispersions to deposit thin TiO_2 films onto indium tin oxide (ITO) coated glass substrates. All these films exhibited only the anatase phase as confirmed by X-ray diffraction analysis. Using the time-of-flight technique, the electron drift mobility in the porous TiO_2 films was measured. The results show that in the low field region ($< 55{,}000\,\mathrm{V\,cm^{-1}}$) the mobility, in all the films, were in the range of 10^{-7} to $10^{-6}\,\mathrm{cm^2\,Vs^{-1}}$. The drift mobility in the films prepared by reactive sputtering was consistently higher than in the films prepared by the two other techniques. Sputter deposited films had lower porosity ($\sim$ 10% and 36% for normal-, and oblique (60°)-angle deposited films) compared to $\sim$ 50% for films deposited by the two other techniques. The relationship between the drift mobility and film morphology is discussed with the aid of scanning electron microscopy studies.

1. INTRODUCTION

The transport of charge carriers in nanoporous semiconductors that are being used in the new generation of solar cells (such as dye sensitised solar cells) is of fundamental importance. The nature of charge transport is determined by the chemical composition and the microscopic structure and morphology of the material [1, 2]. Drift mobilities (μ) in nanocrystalline semiconductors such as TiO_2 may be much lower than in the equivalent single crystalline material [1]. This difference may be attributed to the effects of defects at the grain boundaries and the extremely large surface area of the nano-materials.

In this study we use the time-of-flight (TOF) technique to measure the drift mobility of electrons in nanoporous TiO_2 films prepared by three different techniques, namely: sol-gel synthesis followed by doctor blading ("colloidal" films), electrostatic spray assisted vapour deposition (ESAVD), and oblique-angle DC magnetron sputtering. These methods of deposition provide films of different morphologies.

†Permanent address: Department of Physics, University of Nairobi, P.O. BOX 30197, NAIROBI-KENYA
E-mail: boaduda@uonbi.ac.ke

2. EXPERIMENTAL

The ESAVD technique involves spraying atomized precursor droplets across an electric field where the droplets undergo decomposition and/or chemical reaction in the vapour phase close to the heated substrate. The details of film preparation used here are similar to those reported elsewhere [3]. The colloidal TiO_2 film of 4.0 microns thickness was prepared by the doctor blading the TiO_2 colloidal paste onto an ITO conducting glass substrate. The paste was then sintered at 450°C for 30 minutes to remove the polymeric binder (polyethylene glycol (PEG)), and also create a continuous network of nanoparticles. The DC reactive magnetron sputtered samples were prepared under the following conditions: base pressure was 2×10^{-5} Torr, argon pressure was 4×10^{-3} Torr, current of 6 A (400 V) was applied to the titanium target (99.99% purity). The deposition time was 140 minutes. The oxygen was controlled by an optical emission (OEM) feedback loop by controlling the degree of poisoning of the titanium target. The TiO_2 films were stable at 25% of the original metal emission value. Two sets of films were sputter-deposited; (i) normal angle incidence (SD90) and (ii) 60°-oblique angle incidence (SD60) between the plane of the substrate and the direction of the molecular

beam. All the films prepared by the three different techniques were deposited on ITO coated conducting glass substrates (work function 4.7 eV) having a resistance/square of 15 Ω. The thickness of all the films was measured by a Tencor Alpha-Step 200 profilometer. The porosity of the anatase TiO_2 films was estimated using the weighing method, i.e., the substrates were weighed before and after deposition of the films. From the dimensions of the film (substrate surface area and thickness of the film) the bulk densities and hence porosities were determined, using 3.9 g cm^{-3} [4] as the theoretical density of anatase TiO_2.

X-ray diffraction (XRD) characterizations were conducted using a Philips PW1700 Series Automated powder diffractometer with CuK_α (λ = 0.15405 nm) radiation from a secondary crystal monochromator (in Bragg-Brentano configuration, accelerating voltage = 40 kV and current = 40 mA). The surface and cross section of the thin films were studied by a high-resolution scanning electron microscope (LEO 1525).

In the TOF technique the sample is subjected to an electric field produced by a bias voltage across blocking electrodes on opposite surfaces. A short pulse of light is flashed upon the sample through one electrode, which is semitransparent. The photon energy should exceed the bandgap of the material and the optical absorption coefficient should be sufficiently large that all the light is absorbed within a shallow penetration depth close to the illuminated surface. The large electric field separates the electron-hole pairs created by the absorbed light. The front electrode quickly collects carriers of one sign, while those of the opposite sign are pulled away and drift across the sample, under the influence of the field, to the back electrode.

For TOF experiments, gold contacts (work function 5.1 eV) were evaporated on to the TiO_2 films using a shadow mask. The device area was around 4.2 mm^2. The measurement was performed either in air (colloidal TiO_2) or vacuum (all other films) in a conventional setup. For measurements in vacuum, the chamber was evacuated to approximately 10^{-4} Torr. The carriers were generated with a frequency-trebled Nd:YAG laser (spectral wavelength 355 nm, pulse width less than 6 ns, energy per pulse ~ 7 mJ, repetition rate 1 Hz, and nominal beam diameter 2–8 mm), illuminating through the ITO. A Tektronix TDS 3000 Series digital phosphor oscilloscope was used to capture the photocurrent-time transients. Depending on the polarity of the applied voltage either positive or negative carriers can be drawn into the sample during photoexcitation. The attempt to draw the hole by applying positive voltage to the illuminated transparent electrode was not successful even at very high voltage. This observation suggests that the hole-mobility of porous TiO_2 is very low. A photocurrent transient was observed when negative voltage was applied to the illuminated ITO and therefore the observed photocurrent transient is due to electron. The conducting glass was thus biased negative relative to the gold with a voltage (V_a) in the range 3 to 25 Volts. The applied field was thus given by E = V_a/l, where l is the thickness of the film.

3. RESULTS AND DISCUSSION

3.1. Results. Whereas the ESAVD TiO_2 films were milky in colour, and sol-gel based TiO_2 films were transparent, the sputtered TiO_2 films appeared slightly dark grey. This greyish colour has also been previously observed for [low oxygen-argon ratio (0.050)] sputtered TiO_2 [5], and is said to be typical of rutile TiO_2 with a high density of electrons in the localised states, due to oxygen vacancies. Oxygen deficient anatase TiO_2 is also known to have a darker colour [6]. The sputtered TiO_2 lost its grey colour when heat-treated in air at 500°C for 30 minutes, as expected upon oxidation of reduced TiO_2. The milky colour in the case of the ESAVD film is due to the large (micron sized) particle size, causing strong scattering of visible light, while the small (20–50 nm) particle size in the sol-gel films cause negligible scattering. X-Ray diffraction analysis (see Figure 1) of all the samples indicated that they comprised mainly anatase with little (sputtered) or no rutile phase detected. From the widths of the reflection line A(101), we can infer that the crystallites of the colloidal TiO_2 was the finest, with those of the sputtered TiO_2 being the coarsest.

The ESAVD film had average thickness of 3.4 μm and ~ 50% porosity, whilst the colloidal based film was 4.0 μm thick and ~ 50% porous. The SD90 film had an average thickness of 4.7 μm and porosity ~ 10%, while the SD60 film was 4.6 μm thick and ~ 36% porous. The difference in porosity of the two sputter deposited films could be explained when we consider that during oblique-angle deposition some areas of the substrate are shielded or shadowed by the initial island growth of the evaporated material resulting in more porous structure. Figure 2 shows typical micrographs (surface and edge) of the ESAVD, colloidal and sputtered TiO_2 films. Notable is the high porosity but quite large particles (> 500 nm) of the ESAVD film deposited at 500°C, compared to those in the colloidal film (~ 20–50 nm). The sputtered films show columnar structure with film deposited at 60° showing columns with narrower widths compared to those comprising the film deposited at normal angle. Recent studies [7] have also shown that columnar structure can be obtained using the ESAVD technique by careful tailoring of the deposition conditions.

Figure 3 shows a log-log plot of a typical photocurrent transient. Although the transient is highly dispersive, it does not show the asymptotic power-law behaviour which is typical of dispersive TOF traces in many materials, and the position of the characteristic "knee," marking the intersection of the short-time

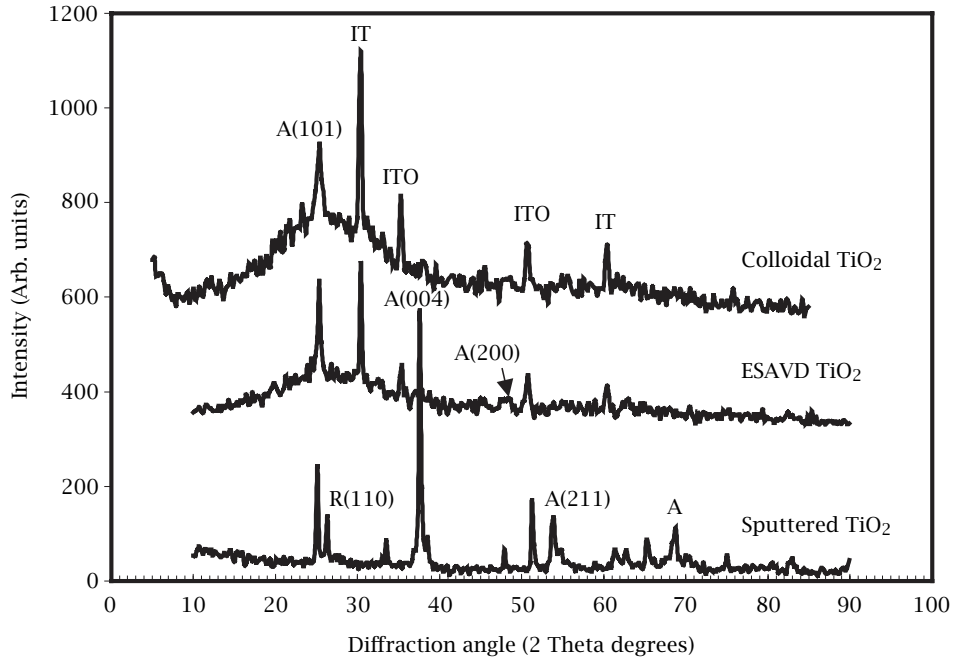

Figure 1. *X-ray diffraction patterns of* TiO_2 *films prepared different techniques on ITO coated glass substrates: (1) DC magnetron sputtering (2) electrostatic spray assisted vapour deposition (ESAVD) (3) doctor-blading of colloidal* TiO_2. *The* TiO_2 *films are basically anatase (A) though minute presence of rutile (R) was detected in the sputtered films.*

and long-time asymptotes on a log-log scale, is hard to define. Therefore we used two methods to determine the transit time, t_r. The first was to estimate the position of the knee, and the second was to find the time at which the gradient of the $\log I - \log t$ plot equals -1, as shown. The two methods will clearly agree to within a small error in the case of a transient with well-defined asymptotes. The resulting values of t_r differed by less than 20% and consequently we remark that this simpler method may be an adequate means of estimating the characteristic transit time in very dispersive materials.

The lack of clear short-time and long-time asymptotes in the transients is not a cause for concern. A power-law asymptotic tail is formally expected only in the case of dispersive transport through an exponential density of trap states, which may not apply for these materials. More importantly, electron hole recombination, if present, will tend to make the signal decay faster than expected. We show later that our films may be incompletely depleted, and in those conditions recombination is expected to be important. Finally, we refer to the work of Dittrich et al. [12] for similar photocurrent transients on TiO_2 films also prepared by the sol-gel procedure, and point out the non-power-law behaviour of those transients.

The photocurrent transients shift to shorter times with increasing applied bias as expected. This proves that the observed transient is indeed due to a drift current and not to some other phenomenon. The drift mobility values derived from

$$\mu = \frac{l^2}{V_a t_r} \tag{1}$$

where l is the sample thickness, and V_a the applied bias, are shown Figure 4. The electron drift mobility of the colloidal and ESAVD films was generally lower than for the sputtered films. Note that although the drift mobility values of colloidal TiO_2 film were obtained in air (the other films were measured in vacuum) the photocurrent transients in vacuum were much slower, so these values may be considered an upper limit. It is important to point out that there was no significant difference between the electron mobility values of the sputter deposited films (SD90 and SD60), indicating that in these films the effect of porosity was comparatively small. Since the films prepared by the ESAVD and colloidal techniques had similar porosity ($\sim$ 50%), the slightly higher mobility values of the ESAVD films may be attributed to the larger particles, hence fewer grain boundaries, observed in this film. The apparent field dependence of the mobility is discussed in the next section.

3.2. Discussion. Our drift mobility values of the tested anatase TiO_2 are of the same order of magnitude (7×10^{-6} cm^2/Vs) as those obtained previously for screen-printed colloidal anatase TiO_2 (particle diameter 16 nm) measured using TOF [1, 8] while lower than the

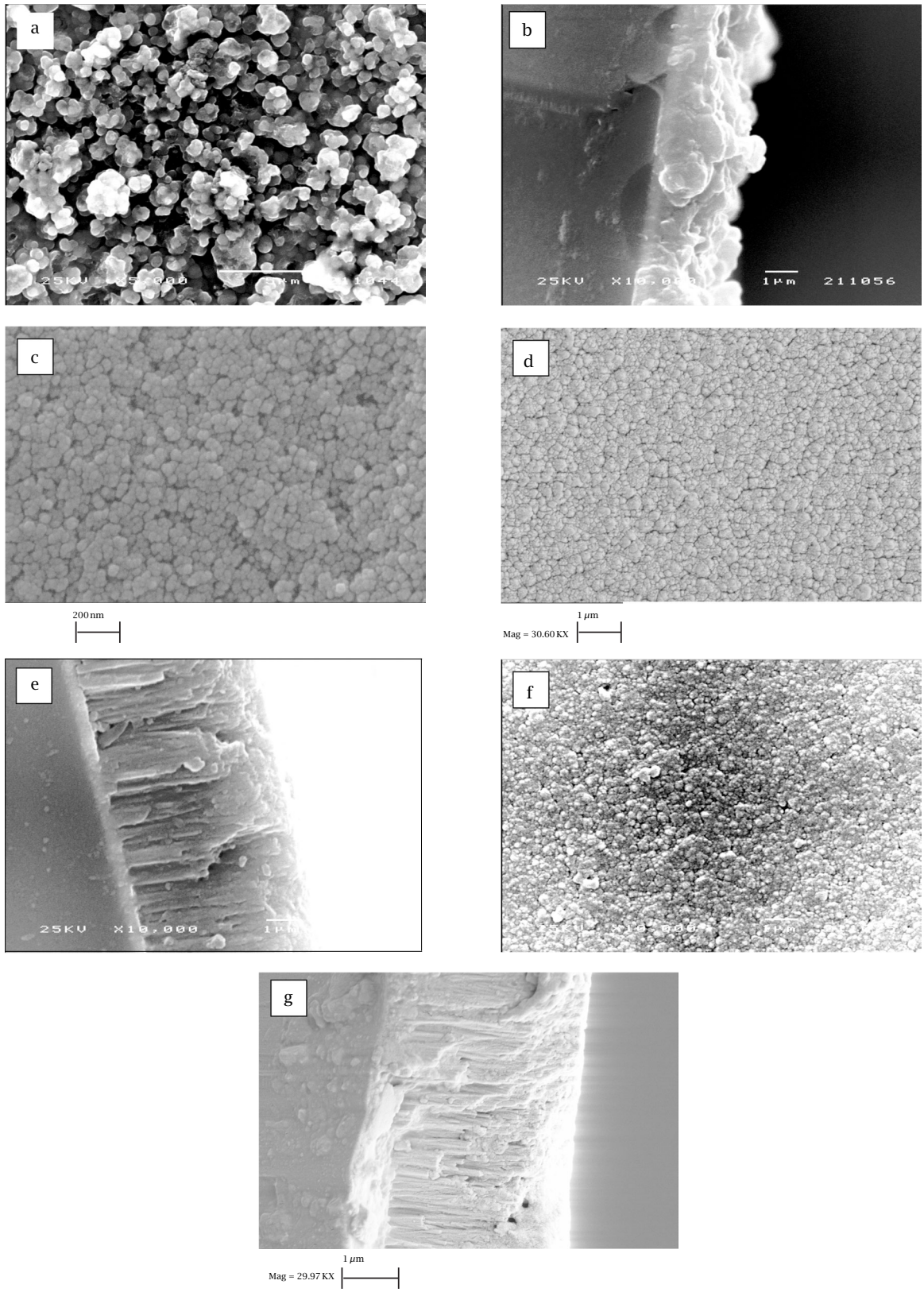

Figure 2. *The SEM micrographs of the* TiO_2 *films prepared by different techniques: Electrostatic spray assisted vapour deposited film (a) surface, (b) edge; Colloidal film (c) surface; Sputter deposited- oblique angle* 60*-degrees (d) surface (e) edge; Sputter deposited- normal angle (f) surface (g) edge.*

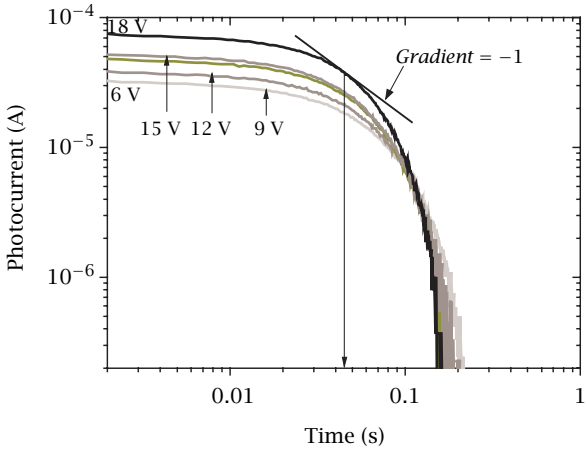

Figure 3. *Typical log-log plot of photocurrent response for electrons in porous* TiO_2 *(in this case colloidal* TiO_2*, average thickness* 4.0 μm*).*

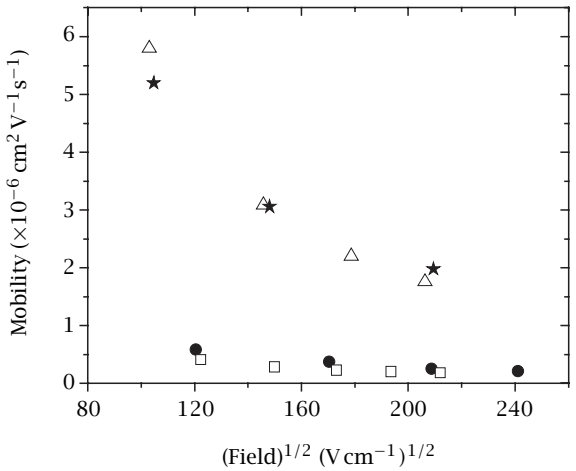

Figure 4. *The electric-field dependence of drift mobility in porous* TiO_2 *films prepared by different techniques. Contrary to the expected behaviour, the mobility appears to decrease with increasing electric field: ESAVD (filled circles) Colloidal (open squares), Sputtered, normal-angle (open triangles), Sputtered,* 60° *-oblique angle (filled stars).*

value 6×10^{-4} cm^2/Vs deduced from the effective diffusion coefficient for transport in electrolyte contacted colloidal TiO_2 films [9]. The room temperature electron drift results of these porous anatase TiO_2 are, however, much lower than 4 cm^2/Vs [10] or $\sim$ 20 cm^2/Vs (in non-stoichiometric TiO_2) [11] in large single crystals of anatase TiO_2.

The mobility value of sputter deposited TiO_2 (5.6×10^{-6} cm^2 V^{-1} s^{-1}) is one order magnitude higher than the other two films. The lower electron drift mobility in the colloidal and ESAVD films compared to the sputtered ones can be attributed to their observed high porosity, smaller grain size with increased grain boundary and surface area, compared to that of sputter deposited TiO_2 films. The columnar rod-shaped particles of the sputtered films reduce the number of particle-particle hops required for charge transfer to the substrate, thus enhancing the chances of an electron moving through the electrode without recombining or being trapped.

The decrease of mobility with field (in the low field region) as observed in these results is still less well understood. Dittrich et al., [12] have reported that the value of μ is practically independent of applied bias voltage (V_a) for V_a < 10–15 V, but for higher V_a the drift mobility (μ) starts to decrease. It is normally expected that the mobility should be field-independent, or possibly *increase* with electric field in the case of a field assisted hopping mechanism. Takashima et al. [13] have reported for poly(alkylthiopene) films of various alkyl chain lengths an initial negative field-dependent mobility at low fields. They proposed that in Schottky junction semiconductor structures, at applied biases smaller than some critical value V_c, the external bias is mainly dropped across a depletion layer of field-dependent thickness d, leaving a field-free "bulk" region of thickness $(l-d)$ connected to the ohmic contact. (In our case, the depletion layer is expected to form next to the interface between the negatively charged gold contact and the n-type TiO_2.) The depleted region has a low conductivity σ_d relative to that of the undepleted bulk material, σ_b (i.e., $\sigma_d \ll \sigma_b$). The apparent transit time (t_r) of the carriers can then be approximated by

$$t_r = \frac{[1 + (\frac{\sigma_b}{\sigma_d})(\frac{d}{l})]l^2}{\mu V_a} \tag{2}$$

so that the effective bias (V_{eff}) experienced by the carriers is

$$V_{\text{eff}} = \frac{V_a}{[1 + (\frac{\sigma_b}{\sigma_d})(\frac{d}{l})]} \tag{3}$$

where $d = (2\varepsilon\varepsilon_o/en_o)^{1/2}(|V_a - V|)^{1/2}$, ε is the dielectric permittivity, ε_o is the permittivity of free space, n_0 the equilibrium carrier density, e the electronic charge and V the Schottky barrier height or built-in bias. (In TOF experiments, V_a is normally > V_c), V_c is the bias at which the film is just depleted and is given by $V_c = en_o l^2/2\varepsilon\varepsilon_o + V$. As bias is reduced below V_c, d decreases and the transit time increases more slowly than $1/V_a$, with the effect that the mobility, defined from $\mu = l^2/V_{\text{eff}}t_r$, appears to decrease. Thus the negative-field dependence of μ in the low field region can be attributed to the bias dependent depletion width.

Juska et al. [14] proposed a similar explanation for negative field-dependent mobility in the low field region as measured by TOF. They argued that high equilibrium carrier densities and the resulting redistribution of electric field inside the sample cause the transit time to

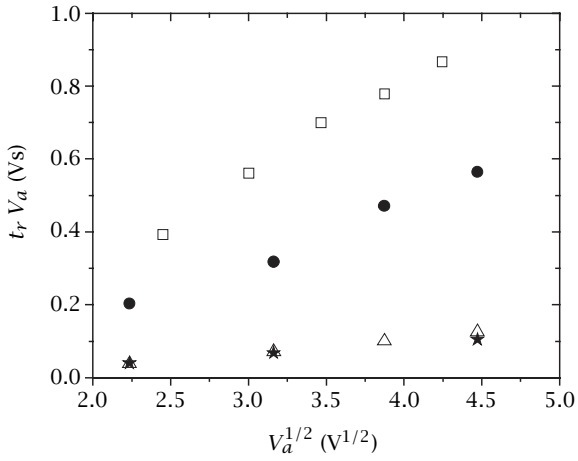

Figure 5. *The plot of $t_r V_a$ versus $V_a^{1/2}$ for porous* TiO_2 *(anatase) prepared by different techniques: ESAVD (filled circles) Colloidal (open squares), Sputtered, normal-angle (open triangles), Sputtered,* 60°*-oblique angle (filled stars).*

exceed the dielectric relaxation time ($t_d = \varepsilon\varepsilon_o/(ep_o\mu)$) and the necessary condition for TOF, ($t_d \gg t_r$) may not fulfilled. The apparent mobility approaches the true mobility only when $V_a \gg V_c$.

To test whether our samples lie in the regime of negative apparent mobility we evaluate V_c. Substituting the values $\varepsilon = 114$, $n_o \sim 10^{16}\,\mathrm{cm}^{-3}$ [15] and $l = 4.7\,\mu$m, we get $V_c = 18$ V. This may be considered a lower limit since lower values of ε [16] and of n_o [17] have been reported for anatase. This value of V_c is comparable to the applied voltages (V_a = 3–25 V) used during the experiments and so the criterion for accurate mobility measurement by TOF ($V_a \gg V_c$) is not satisfied. Under these circumstances, our results may be explained and the true mobility estimated using Takashima's model. If the barrier height $V \ll V_a$ ($V \sim 0.4$ V for ITO/TiO_2/Au), so that $d \propto V_a^{1/2}$ Takshima's [12] expression for t_r can be written

$$t_r V_a = \Psi V_a^{1/2} + l^2/\mu \qquad (4)$$

where Ψ is a constant given by $\Psi = \frac{\sigma_b l}{\sigma_d}(\frac{2\varepsilon\varepsilon_0}{en_0})^{1/2}$. Shown in Figure 5 are plots of $t_r V_a$ vs. $V_a^{1/2}$ for the TiO_2 films deposited by the different techniques. The linear behaviour confirms that eq. (4) is followed for our samples. The mobility values of the various TiO_2 films estimated from the intercepts are: $6.6 \times 10^{-7}\,\mathrm{cm}^2\,\mathrm{V}^{-1}\,\mathrm{s}^{-1}$ (electrostatic spray assisted vapour deposited), $6.8 \times 10^{-7}\,\mathrm{cm}^2\,\mathrm{V}^{-1}\,\mathrm{s}^{-1}$ (colloidal TiO_2) and $5.6 \times 10^{-6}\,\mathrm{cm}^2\,\mathrm{V}^{-1}\,\mathrm{s}^{-1}$ (sputter deposited TiO_2). These values are comparable to those obtained from eq. (1). Note that neither this linear behaviour nor the values of the mobility extracted are a function of the values of n_0 and ε assumed in the calculation of V_c.

The theory could be tested, in principle, by applying higher electric fields so as to completely deplete the film and enter the regime where t_r is unaffected by depletion. Although higher V_a could not be applied with our current apparatus and thinner films were not available, this could be addressed in a future study. It is also useful to improve the values of n_0 and ε used by complementary studies of the electrical behaviour of these materials, and thereby qualify the value of V_c extracted. Studies are in progress along these directions.

4. CONCLUSION

In summary we note that the electron drift mobility measured by TOF technique for porous TiO_2 is in the range of 10^{-7} to $10^{-6}\,\mathrm{cm}^2\,\mathrm{V}^{-1}\,\mathrm{s}^{-1}$, and is dependent on the morphology of the film. Columnar TiO_2 films have higher electron drift mobility than porous films with random distribution of TiO_2 particles. This could be due to the fact that charge carriers in the columnar films, with the columns aligned nearly in the direction of the field, may be able to gain kinetic energy from the applied field along the column axis which minimises recombination and scattering, resulting in higher mobility.

ACKNOWLEDGMENTS

The authors wish to thank Dr. Xianghui Hou, and Dr. Jo Hamphsire who prepared the EASVD, and sputtered thin films respectively. Further, they are grateful to James R. Durrant for providing the colloidal TiO_2 paste and to Saif A. Haque and Theo Kreouzis for their technical assistance. BOA and PR acknowledge the Association of Commonwealth Universities for Commonwealth Fellowship and Scholarship respectively. JN acknowledges the EPSRC for award of an Advanced Research Fellowship.

REFERENCES

[1] T. Dittrich, Phys. Stat. Sol. (a) **182** (2000), 447.
[2] J. A. Anta, J. Nelson, and N. Quirke, Phys. Rev. B **65** (2002), 125324.
[3] K. L. Choy and B. Su, J. Mater. Sci. Lett. **18** (1999), 943.
[4] G. Szczyrbowski, G. Brauer, M. Ruske, J. Bartella, J. Schroeder, and A. Zmelty, Surface and Coatings Technology **112** (1999), 261.
[5] M. M. L. Gomez, Photoelectrochemical and Physical Properties of Sputter Deposited Titanium Oxide Electrodes: A New Option for Dye-sensitised Nanocrystalline Solar Cells, Ph.D. Thesis, Faculty of Science, University of Lima, (2001) p. 124–129.
[6] K. Takeuchi, I. Nakamura, O. Matsumoto, S. Sugihara, M. Ando, and T. Ihara, Chemistry Letters **12** (2000), 1354.
[7] J. D. Vyas and K. L. Choy, Mater. Sci. & Eng. A **277** (2000), 206.

[8] T. Dittrich, E. A. Lebedev, and J. Weidmann, Phys. Stat. Sol. (a) **165** (1998), R5.

[9] A. Solbrand, A. Henningsson, S. Sodergren, H. Lindstrom, A. Hagfeldt, and S.-E Lindquist, J. Phys. Chem. B **103** (1997), 1078.

[10] H. Tang, K. Prasad, R. Sanjines, P. E. Schmid, and F. Levy, J. Appl. Phys. **75** (1994), 2042.

[11] L. Forro, O. Chauvet, D. Emin, L. Zuppiroli, H. Berger, and F. Levy, J. Appl. Phys. **75** (1994), 633.

[12] T. Dittrich, J. Weidmann, V. Y. Timoshenko, A. A. Petrov, F. Koch, M. G. Lisachenko, and E. A. Lebedev, Mater. Sci. & Eng. B **69–70** (2000), 489.

[13] W. Takashima, S. S. Pandey, T. Endo, M. Rikukawa, and K. Kaneto, Current Applied Physics **1** (2001), 90.

[14] G. Juska, K. Genevicius, K. Arlauskas, R. Osterbacka, and H. Stubb, Phys. Rev. B **65** (2002), 233208.

[15] G. Rothenberger, D. Fitzmaurice, and M. Gratzel, J. Phys. Chem. **96** (1992), 5983.

[16] R. J. Gonzalez and R. Zallen, Phys. Rev. B **55** (1997), 7014.

[17] S. A. Studenikin, N. Golego, and M. Cocivera, Semicond. Sci. Technol. **13** (1998), 1383.